Meso-scale simulation of the post-cracking behavior of hybrid industrial/recycled steel fiber-reinforced concrete

A. Caggiano[1], D. Said Schicchi[2], E. Martinelli[3] and G. Etse[1]

ABSTRACT: This paper aims at investigating the mechanical behavior of concrete reinforced with Recycled Steel Fibers (RSFs) recovered from waste tires. The results of an experimental activity carried out on Fiber-Reinforced Concretes (FRCs), obtained by mixing Industrial Steel Fibers (ISFs) and RSFs are briefly presented. After this, the paper focuses on the formulation of a numerical model capable to simulate the stress-crack opening displacement of FRC. Particularly, FRC is assumed as a multi-phase material, where the nonlinear material behavior of the concrete matrix is modelled by means of a discrete-crack approach for meso-scale analysis. ISFs and RSFs are assumed as embedded short beams randomly distributed within the meso-scale matrix. The internal forces in the steel fibers are obtained from both the bond-slip and dowel actions reproduced by fiber effects crossing cracks. Comparisons between experimental results and numerical predictions are discussed and analyzed.

1 INTRODUCTION

In recent years the disposal of exhaust tires has emerged as a big issue in waste management, as the increasing amount of these waste represents a serious threat for both environment preservation and human health. Based on the "Council Directive 1999/31/EC" of the European Commission on the Landfill of Waste, as of 2003 post-consumer "whole tires" may no longer be landfilled and, since July 2006, such regulations must be applied to both "whole" and "shredded" tires. Therefore, there are strong motivations for recycling waste tires, which can easily be turned into an eco-friendly source of secondary raw materials (Sienkiewicz et al., 2012).
Recycling processes of waste tires mainly consist of separating the internal steel reinforcement from the rubber covering. Rubber scraps and short steel fibers are obtained via these processes and, among other alternatives, they can be employed in partial-to-total replacement of ordinary concrete constituents. For example, rubber scraps find an interesting field of application as a partial replacement of ordinary stone aggregates for obtaining the so-called "rubberized" concretes (Centonze et al., 2012). Furthermore, Recycled Steel Fibers (RSFs) can replace Industrial ones (ISFs) for producing cementitious composites generally referred to as RSF-Reinforced Concretes (Graeff et al., 2012).
Various experimental studies, available in the scientific literature, deal with the mechanical characterization of FRC in post-cracking range. Recently issued papers have investigated the mechanical performance and, specifically, the post-cracking response of the most common composite materials, i.e., Steel-FRC (Caggiano et al., 2012), Polypropylene FRC (Elser et al., 1996) or Hybrid-FRC (Banthia et al., 2014). Some experimental campaigns on "ecofriendly FRCs", such as those made with either RSFs obtained from waste tires (RSFRC) (Martinelli et al., 2015) or Natural Fibers (NFRC) by de Andrade Silva et al. (2010) are also available in literature.
Plenty of theoretical models, intended to simulate the failure behavior and post-cracking response of FRC at both material and structural levels, are also available in the literature. They range from empirical design relationships (Nataraja et al., 1999) to more complex meso-mechanical models (Caggiano et al., 2016; Cunha et al., 2012). The latter take into account explicitly the interaction among the different phases of the composite (i.e., fibers, matrix, coarse aggregates and their interfaces) and, hence, require a sound knowledge of fiber-matrix interactions and mechanisms.

This work proposes a meso-scale model aimed at simulating the failure behavior and post-cracking response of Hybrid Industrial/Recycled Steel Fiber-Reinforced Concretes (HyIR-SFRCs). A zero-thickness interface model for plain concrete is employed in the framework of a discrete-crack approach. This discontinuous proposal assumes a fracture-based model originally proposed by Carol et al. (1997). Moreover, a novel and promising approach to account for the fiber effect in concrete composites and mortar has been adopted in this paper. Particularly, this new advanced extension deals with the assumption that ISFs and RSFs can be considered as embedded short elements randomly distributed within the concrete matrix.
The paper is organized as follows. Section 2 reports the main assumptions of the FRC modeling and approaches. Section 3 gives an overview of an experimental campaign of HyIR-SFRCs. Then, Section 4 shows the relevant application of the proposed model for simulating the post-cracking response of the tested HyIR-SFRC specimens. Finally, some concluding remarks are given in Section 5.

2 OUTLINE OF THE MODELING APPROACH

The present model for FRC is inspired to a discrete-crack approach and considers fibers, modeled as beam elements and "embedded" within the concrete matrix. The model formulation includes and combines three internal "sub-formulations".
Firstly, a *fracture energy-based plasticity formulation* for plain mortar/concrete joints was considered. Table 1 summarizes its main features, whereas further details are available in Caggiano and Etse (2015).

Table 1. Overview of the interface model for plain concrete and mortars.

	Fracture - based energy interface model
Constitutive relationships	$\dot{\mathbf{u}} = \dot{\mathbf{u}}^{el} + \dot{\mathbf{u}}^{cr}$ $\dot{\mathbf{u}}^{el} = \mathbf{C}^{-1} \cdot \dot{\mathbf{t}}$ $\dot{\mathbf{t}} = \mathbf{C} \cdot \left(\dot{\mathbf{u}} - \dot{\mathbf{u}}^{cr} \right)$
Yield condition	$f\left(\mathbf{t}, \kappa\right) = \sigma_T^2 - (c - \sigma_N \tan\phi)^2 + (c - \chi \tan\phi)^2$
Flow rule	$\dot{\mathbf{u}}^{cr} = \dot{\lambda}\mathbf{m}$ $\mathbf{m} = \mathbf{A} \cdot \mathbf{n}$
Cracking work-evolution	$\dot{\kappa} = \dot{w}_{cr}$ $\dot{w}_{cr} = \sigma_N \cdot \dot{u}^{cr} + \sigma_T \cdot \dot{v}^{cr} \quad \sigma_N \geq 0$ $\dot{w}_{cr} = \left[\sigma_T - \lvert\sigma_N\rvert tan(\phi) \right] \cdot \dot{v}^{cr} \quad \sigma_N < 0$
Evolution law	$p_i = \left(1 - \left(1 - r_{pi}\right) S[\xi_{p_i}]\right) p_{0i}$
Kuhn - Tucker loading/unloading and consistency conditions	$\dot{\lambda} \geq 0, \quad f \leq 0, \ \dot{\lambda} f = 0$ **Kuhn-Tucker** $\dot{f} = 0$ **Consistency**

The constitutive model for iso-parametric interface elements relates the normal/tangential stress components with the corresponding relative joint displacements; the three-parameter hyperbolic failure surface (Figure 1) by Carol et al. (1997) is assumed as maximum strength criterion while the ratio between spent work and the available fracture (mode I/II) energies controls the post-cracking response.
The internal forces in the steel fibers crossing cracks are obtained by considering the two following mechanical contributions:

i. *Fiber bond-slip effect* developed in the fiber (beam) direction. Pull-out mechanism of steel fibers crossing cracks (these latter represented through opened joints) is formulated by means of a 1-dimensional elasto-plastic model.
ii. *Fiber dowel action* based on elastic foundation ("Winkler beam") concepts to obtain the dowel force-displacement relationship developed in the transversal direction of the considered short beam which crosses an active fracture.

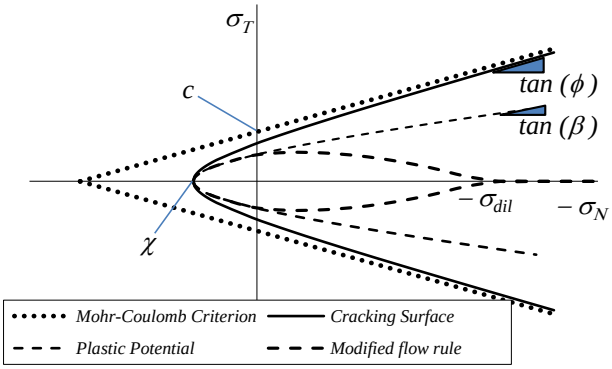

Figure 1. Failure hyperbola by Carol et al. (1997), Mohr-Coulomb surface, plastic potential and modified flow rule.

The description of the complete modelling approach is omitted for the sake of brevity however further details were reported in Caggiano et el. (2016).

3 EXPERIMENTAL CAMPAIGN AND RESULTS

The results reported in this section were obtained from the experimental tests performed at the University of Salerno (Italy) according to UNI-11039-1 (2003) code for definitions, classification and designation and UNI-11039-2 (2003) for the test method.

3.1 Materials and test programme

FRC specimens tested in this study were prepared by adopting a unique mixture for the concrete matrix, which was also employed in preparing the plain concrete specimens considered as a reference (labelled as REF). This mixture was designed for a target *28* days mean cubic compressive strength of *40 MPa* and prepared by using crushed limestone aggregates with a maximum aggregate size of *20 mm* according to EN-12620 (2002) and UNI-11039-1 (2003). A constant cement content of *320 kg/m*^{3} and a free water to-cement-ratio *w/c* of *0.51* were assumed (Martinelli et al., 2015).
Wirand® Fibers type FS7, hereafter referred to as ISFs, were considered along with the RSFs. The key geometric and mechanical properties of ISFs are: l_f *= 33 mm* (fiber length), d_f *= 0.55 mm* (fiber diameter), *AR = 60* (aspect ratio), number of fibers per *kg = 16100*, f_t *> 1200 MPa* (failure strength in tension) and $\varepsilon_u \leq 2\%$ (ultimate strain).
Recycled Steel Fibers (RSFs) employed in this study were supplied by an Italian company whose main business consists in collecting and recycling exhausted tires. As a result of the shredding and separation process, RSFs have variable diameters and lengths, and often are characterized by irregular shapes with curls and twists. Therefore, the description of the main geometric parameters of these fibers deserved a dedicated investigation. Moreover, mechanical characterization tests on RSF through tensile and pull-out tests were carried out at the University of Buenos Aires (Argentina). For the sake of brevity, the report of these results is omitted in this work; further details are available in Caggiano et al. (2015).
The concrete mixtures were prepared by using a laboratory mixer. Both coarse and fine aggregates were saturated and mixed; subsequently, cement, fibers and, finally, a superplasticizer were added. The REF mixture was designed for a target slump value of *150-180 mm*; a value of *175 mm* was actually measured at fresh state. Moreover, the ce-

mentitious matrix composition of all FRC specimens was kept unchanged; only superplasticizer was slightly adjusted for controlling the influence of fibers on workability.
Three cube samples of *150×150×150 mm*^{3} and beam specimens of *150×150×600 mm*^{3} (Figure 2) were cast in polyurethane molds and duly vibrated. One of the cubic samples (labelled as "white") was extracted from each mixture before fiber mixing: it was tested in compression and compared with the corresponding FRC samples with the aim to observe the actual contribution of fibers on the compressive strength in each different mixture. *After 36 h* the concrete samples were demolded. Then, the hardened beam samples were notched (through a *2.0 mm* wide-slit) of *45 mm* depth and starting from the bottom surface of the sample (Figure 2). All concrete specimens were cured in a water bath (*100 %* humidity) at a constant temperature of *22 °C*, up to reach the *28* days of curing.

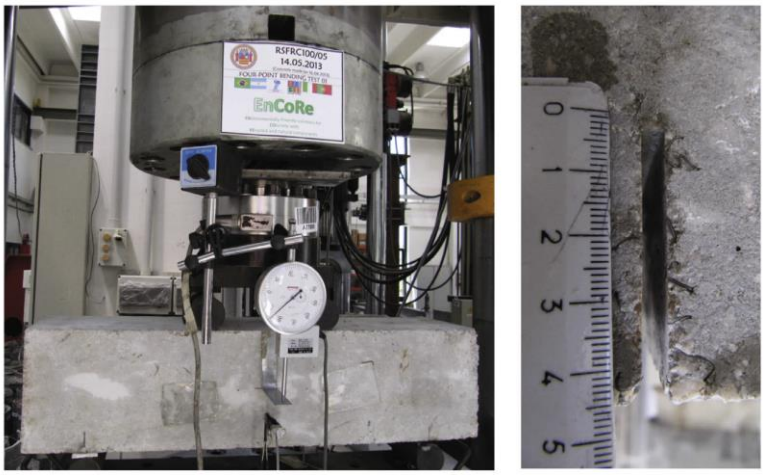

Figure 2. Four-point bending test: experimental set-up and the vertical notch at the bottom surface of the specimen.

Table 2. Considered mixture types of the experimental programme.

Mix Label	Compression (28 days)	Four-point bending test (28 days)
"REF"	3	3
RSFRC 0-05	3	3
RSFRC 25-05	3	3
RSFRC 50-05	3	3
RSFRC 100-05	3	3

Four FRC mixtures were prepared, always using *0.5 %* of fibers in volume of matrix and combining the aforementioned ISFs and RSFs. They were labelled as follows: RSFRC 0-05, with only ISFs (RSFs = 0%); RSFRC 25-05, with 25% of ISFs replaced by an equal amount of RSFs; RSFRC 50-05, with 50% of ISFs replaced by an equal amount of RSFs; RSFRC 100-05 with all RSFs. Table 2 outlines the experimental program reported in this paper.
Four-point bending tests on notched beams (UNI-11039-2, 2003), as shown in Figure 2, were performed in displacement control (adopting a displacement rate of *0.005 mm/s*). Relevant load and displacement quantities were measured and recorded during all tests. Particularly, the crack-tip opening displacements were measured by means of dedicated transducers that monitored the relative displacements of the two sides of the notch tip. Furthermore, compressive tests were performed according to EN-12390-3 (2009) for measuring the cubic compressive strength of the SFRCs at the time of testing.

3.2 Results

Table 3 summarizes the results of *compression tests*: it reports the average values of strength obtained from cubic samples of the plain concrete and FRC mixtures considered in this study. The same table also reports the average values of specific weight measured in hardened samples of the same concrete mixtures. As widely documented in the scientific literature, no significant difference was observed in terms of compressive strengths of both the so-called "white" and SFRC specimens. This means that, at least for the volume fraction considered in this study, the resulting compressive strength of FRC is mainly controlled by the matrix properties. Fibers only play a role in the post-cracking regime.

Table 3. Densities and cube compressive strengths measured in each mixture.

Mix Label	Specific weight [kg/m^3]		$f_{c,cube}$ at 28 days [MPa]	
	white	SFRC	white	SFRC (mean of two)
REF	2371		42.59 (mean of three)	
RSFRC 0-05	2376	2413	40.57	39.01
RSFRC 25-05	2428	2435	36.42	36.52
RSFRC 50-05	2459	2450	36.89	36.74
RSFRC 100-05	2446	2491	36.69	37.37

Four-point *bending* tests were performed with the aim of characterizing the post-cracking flexural behavior of HIRSFRC samples: UNI-11039-1&2 (2003) provisions were taken into account for this purpose.

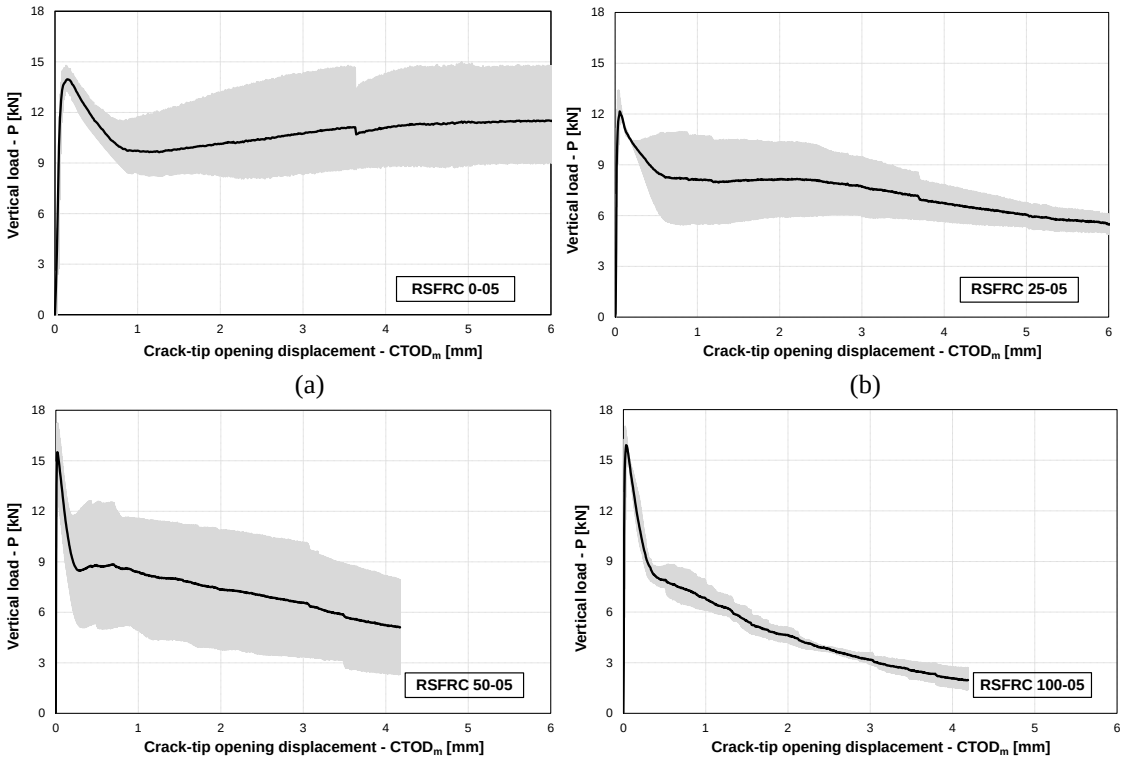

Figure 3. Vertical force vs. CTOD$_m$ curves.

Figure 3 reports the experimental curves of the vertical load, *P*, versus the corresponding Crack Tip Opening Displacement ($CTOD_m$) curves, obtained in the tests: $CTOD_m$ represents the mean of the two opposite $CTOD_s$. Based on the experimental evidence, the post-cracking response in bending of FRC specimens reinforced with only ISFs was characterized by a significant toughness (Figure 3 a), which is due to the bridging action of fibers and cannot be obtained in plain concrete.
The effect of replacing increasing amount of ISFs with an equal quantity of RSFs can be easily understood by analyzing the curves depicted in Figure 3. The post-cracking behavior of FRC is generally characterized by a more pronounced softening range in specimens with a greater quantity of RSFs in substitution of ISFs. This is a result of the lower efficiency of the recycled fibers with respect to the industrial ones, which are specifically designed to exhibit a good interaction with the concrete matrix. Particularly, recycled fibers are not straight, have no hooks and have (generally) lower aspect ratios: these are the main reasons explaining the (expected) decay resulting from replacing part (to total) of industrial fibers with an equal amount (in weight) of recycled ones.
The steeper slope of the post-peak response observed for RSFRC 25-05 (Figure 3 b) is clearly due to the fact that the recycled fibers employed in those specimens need a wider crack opening for mobilizing their bridging effect. The post-peak slope is even steeper for RSFRC 50-05 (Figure 3 c) and RSFRC 100-05 (Figure 3 d) where the actual volume fraction of RSF is even higher. Nevertheless, a significant increase in toughness can be observed for all FRC specimens with respect to the significantly brittle behavior characterizing the post-cracking response of plain concrete.

4 NUMERICAL SIMULATIONS AND COMPARISONS

The experimental results summarized within the previous section are employed for validating a meso-scale model outlined in the present one. More specifically, the model is ntended at simulating the mechanical response of $150\times150\times600\ mm^3$ notched concrete specimens, tested under four-point bending (Figure 4).
Four materials types were considered: plain concrete and HyIR-SFRCs featuring the same fiber quantity (0.5% in volume fraction). The geometry and material properties are chosen according to the tests outlined in Section 3.

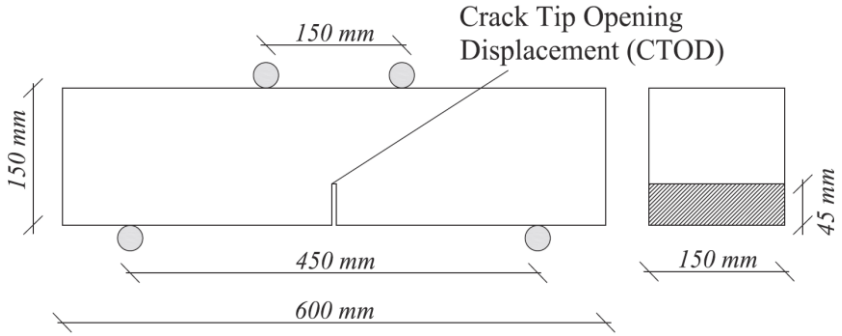

Figure 4. Geometry of the notched beam tested in four-point bending.

The explicit mesoscopic geometry is determined by means of a random 2D generation of both ISFs and RSFs as shown in Figure 5: 20-nodes beam elements, hosted into the continuum mesh as "embedded elements", were adopted for this purpose.
Trusses or beams (or a group of those elements) line embedded in a group of the so-called "host elements" (e.g., the continuous mesh representing the surrounding concrete matrix for FRCC) whose response is used to constrain the translational degrees of freedom of the embedded nodes. Particularly, when a node of an embedded element lies within a host one (becoming an "embedded node"), its translational degrees of freedom are eliminated (i.e., not considered) for the construction of the vector collecting the de-

grees of freedom at global reference. However, the translational degrees of freedom of the embedded node allow to construct the modified stiffness matrix and stresses of the continuous element (when those host an embedded elements), thus influencing in easy way the global solution and equilibrium of the FEM problem.

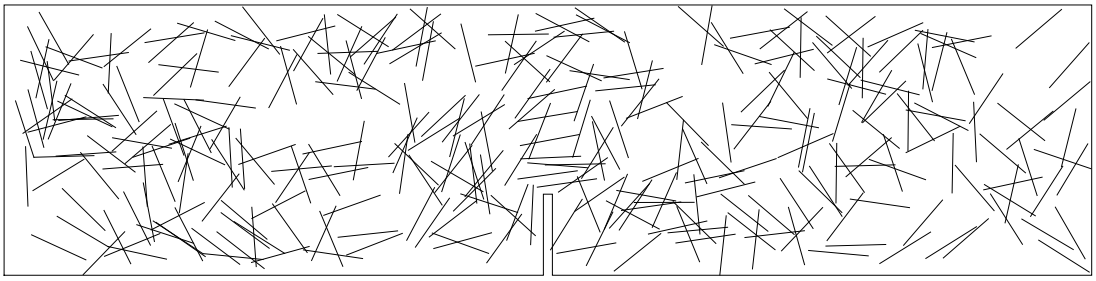

(a) RSFRC 0-05: number of ISFs=316, fiber length ISF=33 mm, diameter ISF=0.55 mm.

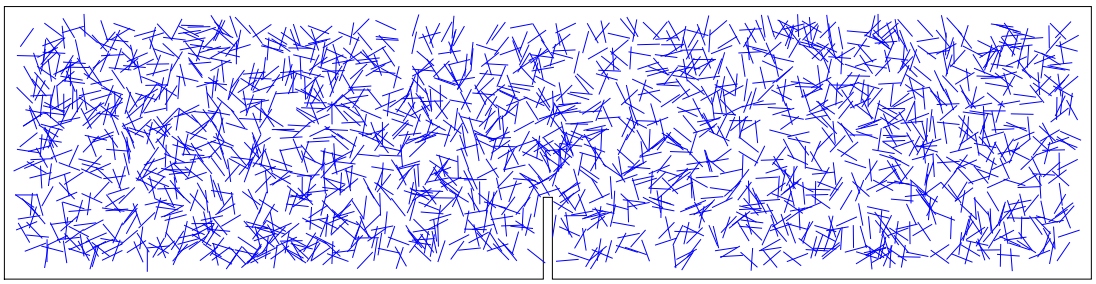

(b) RSFRC 100-05: number of RSFs=2076, fiber length (mean value) RSF=12 mm, diameter (mean value) RSF=0.23 mm (Martinelli et al., 2015).

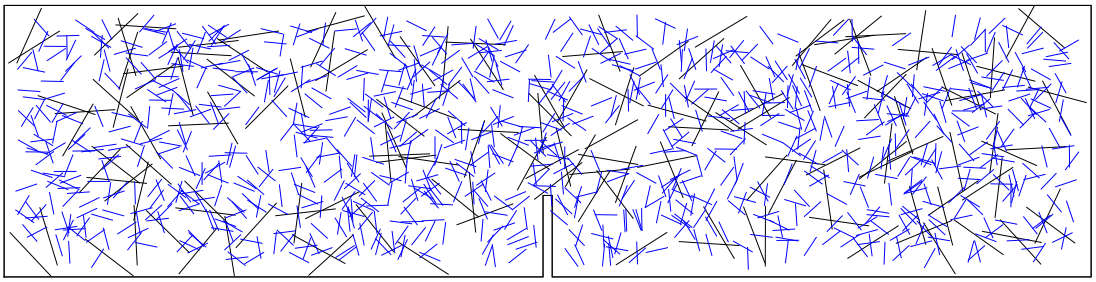

(c) RSFRC 50-05: number of ISFs=158, of RSFs=1038.

Figure 5. Two-dimensional finite element geometry: concrete phases and fibers as embedded short beams.

Figure 6 reports the 2-D geometry of the meso-scale structure considered for the tested specimens and highlights the FE discretization employed in the analyses. Plane stress hypothesis and displacement-based control are assumed. Moreover, 3-node linear elastic plane stress elements have been adopted in the FE mesh, whereas all non-linearities are concentrated within the zero-thickness interface elements defined throughout the adjacent edges of the finite elements in the notch zone. Non-linear fracture-based law and the constitutive models for considering the stress transferred between cracks through the embedded beam elements were introduced according to the formulation outlined in Section 2.

Figure 7 shows the numerical response in terms of vertical load vs. Crack Tip Opening Displacements (CTODs) against the corresponding experimental results. It can be observed that the proposed model leads to very accurate simulations of the post-cracking

response observed in the experimental tests. As expected, the load-CTOD responses of concrete with (Figure 7 b-c-d) or without (Figure 7 a) fibers emphasize the significant influence of fibers on the both peak strength and post-peak response of the FRC specimens tested in bending: the brittle behavior of the concrete matrix became significantly tougher when fibers are added as spread reinforcements.

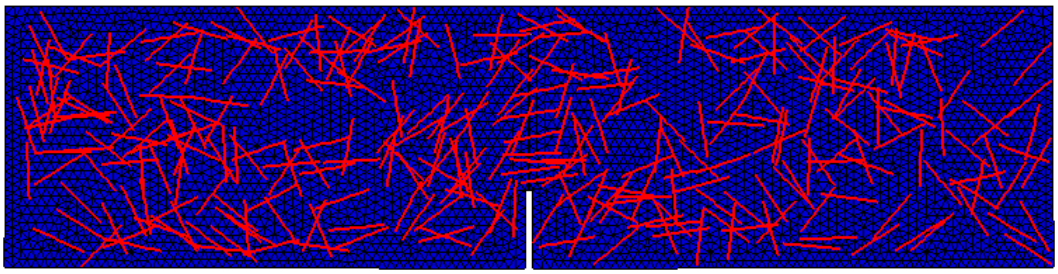

(a) Adopted FE mesh;

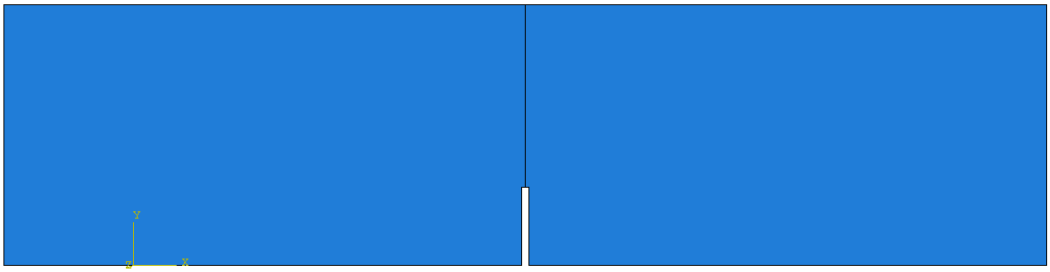

(b) Interface zone at the notch section;

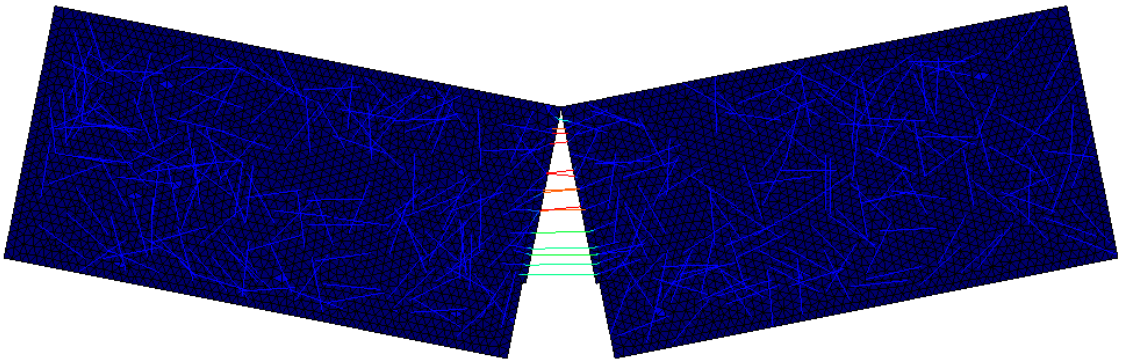

(c) Cracked configuration of the RSFRC 0-05 specimen.

Figure 6. Adopted finite element mesh, interfaces position and possible cracked configuration of the 4-point bending beam. As example there is plotted the results of the RSFRC 0-05 specimen.

The numerical simulations, as well as the experimental observations, confirm that the post-cracking response of FRC specimens with only ISFs (Figure 7 b) is characterized by the highest toughness, as a result of the superior bond properties and dowel action of these fibers with respect to RSFs (Figure 7 d).
The model formulation is also capable to capture the effect of replacing increasing amount of ISFs with an equal quantity of RSFs. Both experimental and numerical results highlight as the post-cracking behavior of FRC is generally characterized by a more pronounced softening range in specimens having a greater quantity of RSFs in substitution of ISFs. It should be noted that the local bond-slip and dowel laws were determined through inverse identification on test results obtained on specimens reinforced with only ISFs and/or RSFs. Numerical predictions of hybrid industrial/recycled steel

fiber-reinforced concrete (i.e., the results reported in Figure 7 c) have been obtained by just changing the fiber types/contents.

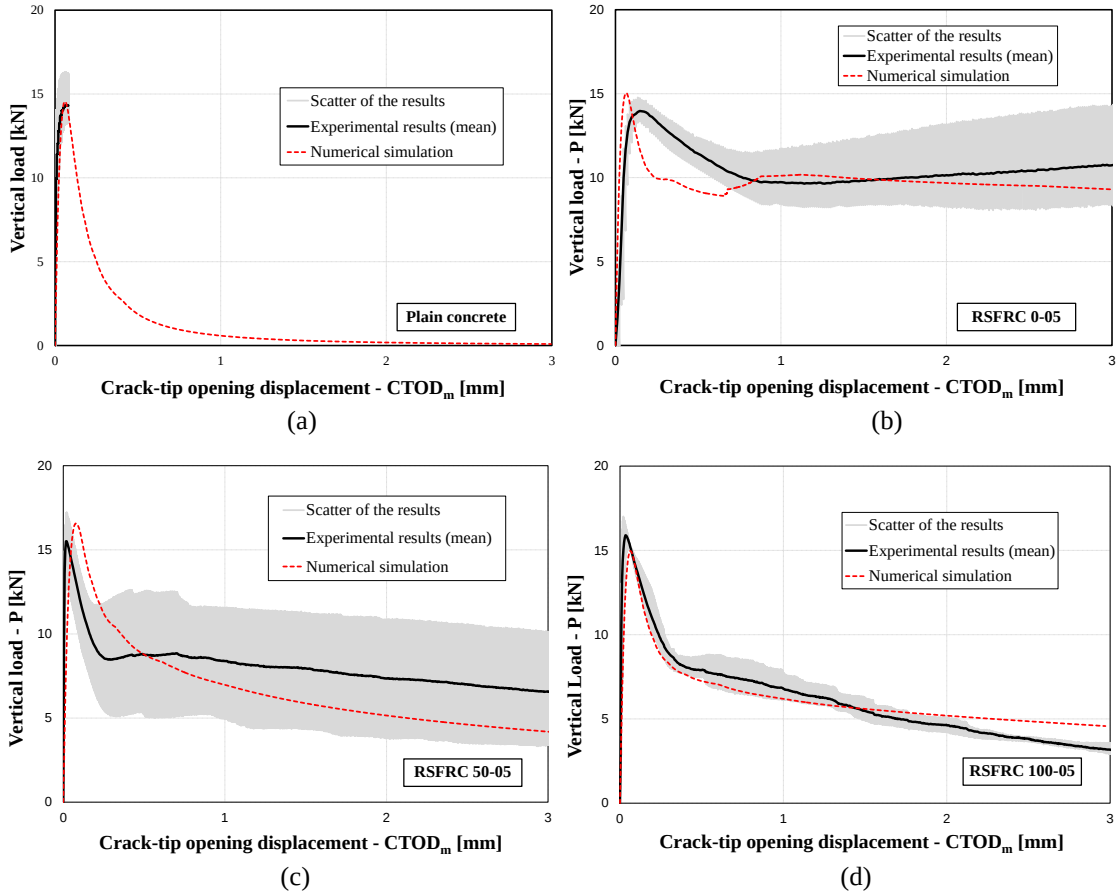

Figure 7. Experimental data vs. numerical simulations in terms of vertical force vs. CTOD$_m$ curves.

5 CONCLUDING REMARKS

This paper proposes experimental results and a meso-mechanical model intended at investigating the fracture response of Hybrid Industrial/Recycled Steel Fiber Reinforced Concretes (HyIR-SFRC). It was based on a discontinuous crack finite element approach and assumed fibers randomly dispersed and embedded as discrete beams elements within the FE mesh of the cementitious matrix. The numerical results demonstrated the capability of the proposed model in simulating the experimental observations derived by four-point bending tests on HyIR-SFRC specimens. Specifically, the model is capable to capture the significant influence of steel fiber contents and types on both the maximum strength and post-peak toughness exhibited by the aforementioned specimens.
Finally, although further experimental comparisons are needed for achieving a full validation, the proposed model paves the way toward predicting the fracture behavior of HyIR-SFRC as a result of the mechanical properties and geometric distribution of their key constituents.

ACKNOWLEDGMENTS

This study is part of SUPERCONCRETE Project (H2020-MSCA-RISE-2014, n. 645704): the Authors wish to acknowledge the financial contribution of the European Union as part of the H2020 Programme.

REFERENCES

Banthia, N., Majdzadeh, F., Wu, J. and Bindiganavile, V. (2014). "Fiber synergy in hybrid fiber rein-forced concrete (hyfrc) in flexure and direct shear", *Cem Concr Compos*, 48, 91-97.

Caggiano, A., Cremona, M., Faella, C., Lima, C. and Martinelli, E. (2012). "Fracture behavior of con-crete beams reinforced with mixed long/short steel fibers", *Constr. Build. Mater.*, 37, 832-840.

Caggiano, A., Said Schicchi, D., Etse, G. and Martinelli, E. (2016). "Meso-scale modeling of hybrid industrial/recycled steel fiber-reinforced concrete", In ECCOMAS 2016 – Europ. Congress on Computational Methods in Applied Sciences and Engineering.

Caggiano, A. and Etse G. (2015). "Coupled thermo–mechanical interface model for concrete failure analysis under high temperature". *Computer Methods in Applied Mechanics and Engineering*, 289, 498-516.

Caggiano, A., Xargay, H., Folino, P. and Martinelli, E. (2015). "Experimental and numerical characterization of the bond behavior of steel fibers recovered from waste tires embedded in cementitious matrices", Cement & Concrete Comp., 62, 146-155.

Carol, I., Prat, P. and Lopez, C. (1997). "Normal/shear cracking model: applications to discrete crack analysis". ASCE-J Engrg Mech, 123, 765-773.

Centonze, G., Leone, M. and Aiello, M. (2012). "Steel fibers from waste tires as reinforcement in concrete: a mechanical characterization", *Cons Build Mater*, 36, 46-57.

Cunha, V.M., Barros, J.A. and Sena-Cruz, J.M. (2012). "A finite element model with discrete embed-ded elements for fibre reinforced composites", Comput Struct, 94-95, 22-33.

de Andrade Silva, F., Mobasher, B. and Filho, R.D.T. (2010), "Fatigue behavior of sisal fiber rein-forced cement composites", *Mater Sci Eng: A*, 527(21–22), 5507-5513.

Elser, M., Tschegg, E. and Stanzl-Tschegg, S. (1996). "Fracture behaviour of polypropylenefibre-reinforced concrete under biaxial loading: an experimental investigation", *Compos Sci Technol*, 56(8), 933-945.

EN-12390-3 (2009), *Testing hardened concrete. Part 3: compressive strength of test specimens*. BSI.

EN-12620 (2002), *Aggregates for concrete*, volume Ref. No. EN 12620:2002 E. Europ. Committee for Standardization, Brussels.

Graeff, A.G., Pilakoutas, K., Neocleous, K. and Peres, M.V.N. (2012). "Fatigue resistance and crack-ing mechanism of concrete pavements reinforced with recycled steel fibres recovered from post-consumer tyres", *Eng. Struct.*, 45, 385-395.

Martinelli, E., Caggiano, A. and Xargay, H. (2015). "An experimental study on the post-cracking be-haviour of Hybrid Industrial/Recycled Steel Fibre-Reinforced Concrete", Construction and Building Materials, 94, 290-298.

Nataraja, M., Dhang, N. and Gupta, A. (1999). "Stress-strain curves for steel-fiber reinforced concrete under compression", Cem Concr Compos, 21(56), 383-390.

Sienkiewicz, M., Kucinska-Lipka, J., Janik, H. and Balas, A. (2012). "Progress in used tyres manage-ment in the European Union: a review", *Waste Manag*, 32, 1742-1751.

UNI-11039 (2003), *Steel Fibre Reinforced Concrete – 1. Definitions, Classification and Designation & 2 Test Method to Determine the First Crack Strength and Ductility Indexes*, UNI Editions, Milan, Italy.